Electrowetting on a lotus leaf

Jiang-Tao Feng, Feng-Chao Wang, and Ya-Pu Zhao[a)]
State Key Laboratory of Nonlinear Mechanics (LNM), Institute of Mechanics, Chinese Academy of Sciences, Beijing 100190, People's Republic of China

(Received 13 February 2009; accepted 2 April 2009; published online 24 April 2009)

Electrowetting on dielectrics has been widely used to manipulate and control microliter or nanoliter liquids in micro-total-analysis systems and laboratory on a chip. We carried out experiments on electrowetting on a lotus leaf, which is quite different from the equipotential plate used in conventional electrowetting. This has not been reported in the past. The lotus leaf is superhydrophobic and a weak conductor, so the droplet can be easily actuated on it through electrical potential gradient. The capillary motion of the droplet was recorded by a high-speed camera. The droplet moved toward the counterelectrode to fulfill the actuation. The actuation speed could be of the order of 10 mm/s. The actuation time is of the order of 10 ms. © *2009 American Institute of Physics.* [DOI: 10.1063/1.3124822]

I. INTRODUCTION

Micro-total-analysis systems (μTAS) or laboratory on a chip (LOC) have been widely used in many fields, such as drug delivery, biochemical sensing, chemical analysis, molecular separation, sequencing and synthesis of nucleic acids, environmental monitoring, and others. Especially for biotechnology, μTAS or LOC offers the potential for a highly efficient, simultaneous analysis of a large number of biologically important molecules in genomic, proteomic, and metabolic studies. The manipulation and control of microliter or nanoliter liquids are the basis of μTAS. Several methods for manipulating microdroplets have been proposed, including the use of structured surfaces,[1] thermocapillarity,[2,3] electrochemical effects,[4] and electrostatic actuation.[5]

An electrostatic method was carried out[6–13] for manipulating discrete microdroplets, which is based upon direct electrical control of the surface tension, a phenomenon known as electrowetting (EW). Static EW directly changes the wettability and local contact angle of droplets on the solid surface by changing the electric potential applied to the microelectrode array under the dielectric layer, and thus results in the asymmetric deformation of droplets to realize the actuation and control of droplets. The electrode configurations known as electrowetting on dielectrics[14,15] (EWOD) are applied widely in LOC. A variety of droplet actuation methods have been conducted, including the thermal Marangoni effect,[16] photosensitive surface treatment,[17] surface acoustic wave,[18] liquid dielectrophoresis,[19] and EW.[20–23] Of all those techniques, EW has drawn the most interest due to its simplicity and fast response.

In this sense, EW is one of the most promising techniques to carry out elementary operations on droplets, such as generating, transporting, splitting, and merging,[24–28] but these operations can often be limited by an irreversible behavior. When applied voltage is larger than a certain voltage, the hydrophobic property of the sample surface could not recover completely. This irreversible behavior can be decreased by using a superhydrophobic surface as the dielectric layer. Currently, a superhydrophobic surface[29,30] with a contact angle higher than 150° is arousing the most attention because it will bring great convenience to daily life as well as to many industrial processes. Conventionally, superhydrophobic surfaces have been produced mainly in two ways: One is to create a rough structure on a hydrophobic surface (contact angle greater than 90°), and the other

[a)]Author to whom correspondence should be addressed. Electronic mail: yzhao@imech.ac.cn.

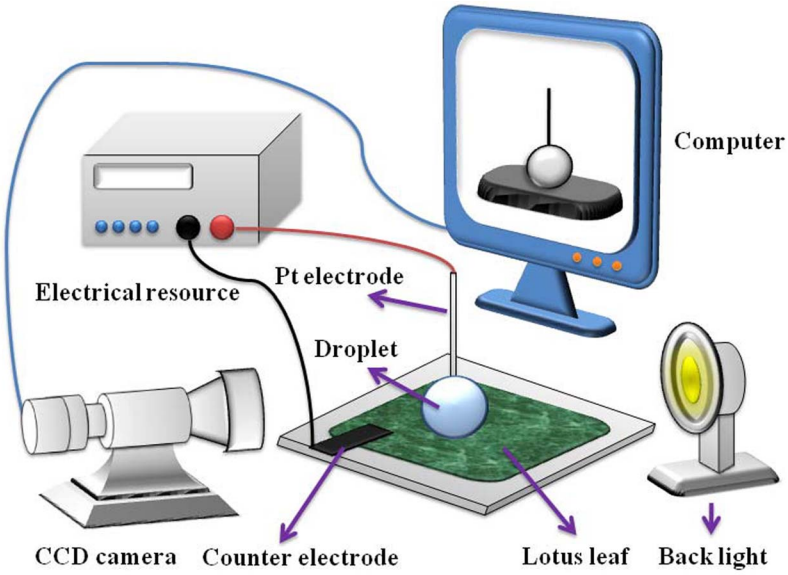

FIG. 1. Sketch of the EW setup, including a wire electrode, a counterelectrode on a moving stage, a dc electrical resource, and the conductive droplet. The external voltage is applied between a thin Pt wire electrode and a counterelectrode.

is to modify a rough surface by a material with low surface free energy. Reversible EW on superhydrophobic surfaces such as Si nanowires[27] has been studied. When the applied voltage is larger than the critical voltage, there still exist irreversible behaviors for EW on the superhydrophobic surface.[27]

Yeo and Chang[31] studied the dynamics of a slender droplet sandwiched between two droplets using lubrication theory and generated a dynamic spreading theory capable of incorporating the contact angle and electric effects upon which EW experiments could be modeled. Yeo and Chang[31] predicted that droplets could be translated or manipulated in many ways through the potential gradient. The possibility of the manipulation and surgery if the droplets, which included drop spreading, translation, and splitting and recombination, was demonstrated using the appropriate tuning of the properties of the bottom potential. Yeo and Chang[31] pointed out that with the advances in micro/nanofabrication techniques, it is now possible to achieve such spatial variation in the electrical potential by patterning electrode surfaces. This has never been experimentally verified.

Because the lotus leaf is superhydrophobic (the contact angle is larger than 150°) and a weak conductor, we study the electrowetting on leaf (EWOL). It is very important to study the droplet actuation on the superhydrophobic surface because of its two outstanding characteristics—a large contact angle and a low contact angle hysteresis. A large contact angle leads to a low contact area and adhesion force between the droplet and superhydrophobic surface; the friction between the droplet and the superhydrophobic surface is small due to the low contact angle hysteresis. Therefore, it is easy for a droplet to move on a superhydrophobic surface due to the low adhesion and friction. We will study the similarities and differences between EWOD and EWOL. The usual EWOD is an equilibrium process in which once the drop reaches the equilibrium contact angle given by the Lippmann equation, no further motion is possible. Thus, the need for electrode arrays, which are sequentially turned on and off successively for drop actuation/translation, occurs in EWOD. EWOL is perhaps another example of spontaneous EW, which has been presented by Yeo *et al.*[32,33] Spontaneous EW, which is a rapid means for the actuation of small liquid volumes in microfluidic devices, can occur spontaneously whereby the contact line continually advances despite the voltage V being held constant in both dc and ac fields. Yeo *et al.*[32,33] framed a spontaneous EW system by parallel line electrode pairs separated by a certain distance. They presented a model that bridged the electrokinetic and wetting hydrodynamic theories to predict the

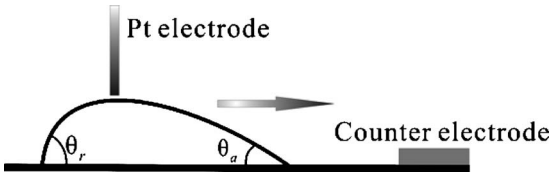

FIG. 2. Actuation of a droplet induced by the Laplace pressure gradient between the two sides of the droplet. θ_a is the advancing angle, and θ_r is the receding angle.

spreading dynamics of these spontaneous EW films for the parallel line electrode configuration. Besides, the principle derived from EWOL could be extended to any poorly conductive, fabricated substrate.

II. EW SETUP

The EW setup shown in Fig. 1 consists of a wire electrode, a counterelectrode on a moving stage, a lotus leaf, a dc electrical resource, a conductive droplet, and a set of OCA20 systems (Dataphysics, Germany, precision of $\pm 0.1°$) to measure the contact angle. A sessile drop method was used to determine the contact angle of water on different surfaces. The moving stage can be shifted to change the electrode leaf distance during our experiment. When an external electrical

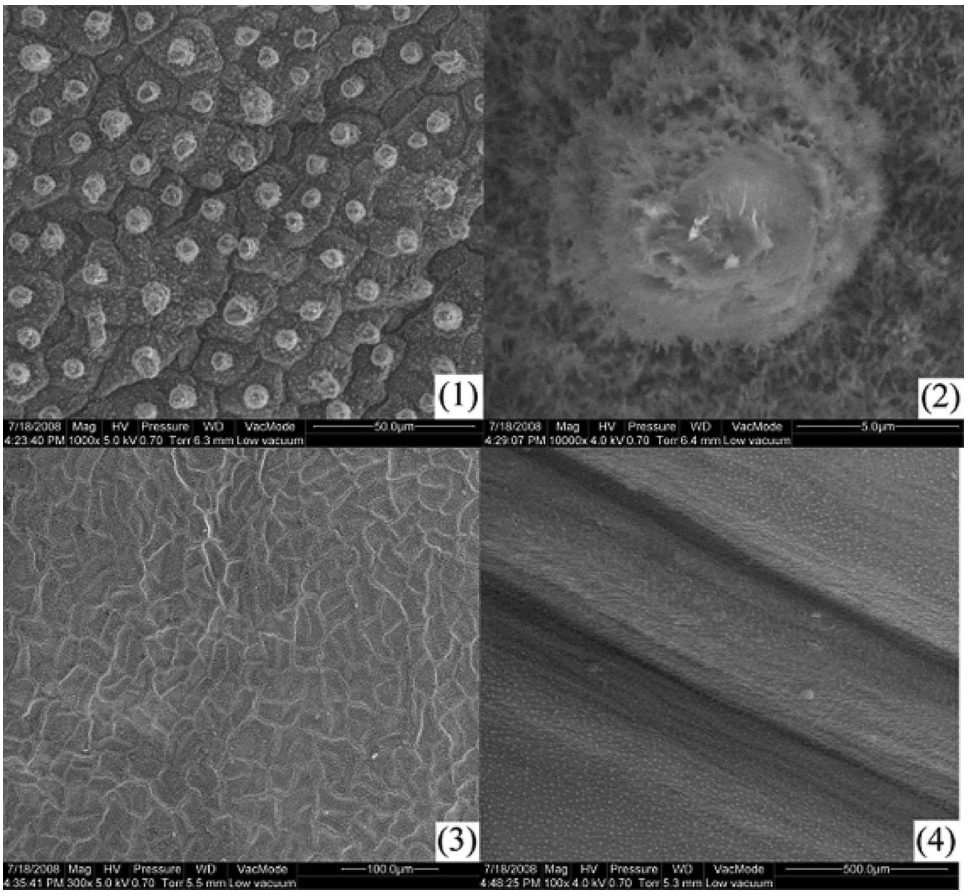

FIG. 3. SEM of the lotus leaf. (1) Upside of the lotus leaf, (2) papilla, (3) back side of the lotus leaf, and (4) the vein. There are many papillae whose radius is about 4 μm on the lotus surface.

TABLE I. Relationship between the distance of two spots on the lotus leaf and resistance.

Spots distance (cm)	Resistance (MΩ)
1	4.16
2	5.86
3	7.47

potential is applied between the two electrodes, the charges redistribute and induce the asymmetric deformation of the droplet to realize the actuation and control of the droplet as shown in Fig. 2.

III. MATERIAL PREPARATION

The scanning electronic microscopy (SEM) images of a lotus leaf (two sides) are shown in Fig. 3. There are many papillae whose radius is about 4 μm on the lotus surface. The lotus leaves are fresh and picked from the Institute of Physics, Chinese Academy of Sciences. The electrical resistance between two spots on the lotus leaf is calibrated by an Ohmmeter and shown in Table I. We can see that the lotus leaf is conductive and has a high resistivity.

The conductive liquid we used is KCl solution (0.1 mol/l). The volume of the droplet is 3 μl. Under this condition, the Bond number $\mathrm{Bo}=\sqrt{g\rho d^2/4\gamma_{lv}}\approx 0.37$, which compares the gravity and surface tension, is smaller than unit (gravity acceleration: $g=9.8$ m/s^2; droplet diameter: $d\cong 2\times 10^{-3}$ m; interface tension: $\gamma_{lv}=72\times 10^{-3}$ N/m; mass density: $\rho\approx 10^3$ kg/m^3; here surface energy and density of water at 25 °C were used). So the influence of gravity is neglected in this paper. The contact angles for lotus and dorsal leaves are 159° and 141°, respectively. An average of six readings was considered as the contact angle of the surface under study.

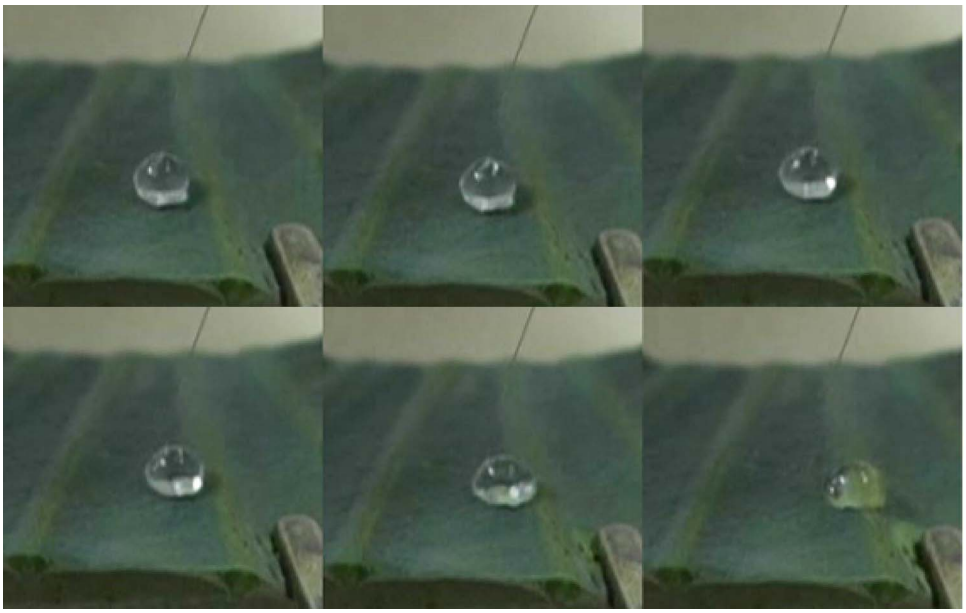

FIG. 4. Video sequence of the moving droplet induced by voltage. The whole process was caught by a Sony camera. The interval of each picture is 200 ms.

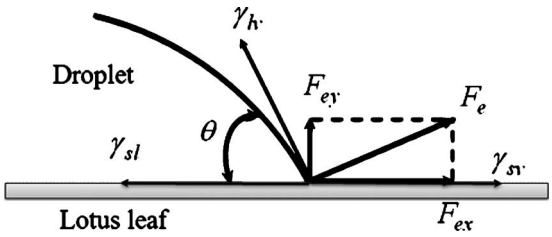

FIG. 5. Influence of the electrostatic force on the horizontal balance of forces acting on the three-phase contact line.

IV. VOLTAGE-INDUCED DROPLET ACTUATION ON A LOTUS LEAF

The situation when voltage is 150 V, as an example, is used to show the process of motion of a droplet induced by applied voltage. Figure 4 shows the whole process caught by a Sony camera; the interval of each picture is 200 ms. It is seen that the droplet climbs up the vein of the leaf. The height of the vein is 1.3 mm.

It has been reported in the literature that the Maxwell stress exerts an outward normal force on the edge of the contact line (Fig. 5).[24,28] The magnitude of the force can be expressed as

$$F_e = \frac{\varepsilon V^2 \csc\ \theta}{2d}, \tag{1}$$

where ε is the dielectric constant of the sample material, θ is the contact angle under the electrical potential V, and d is the thickness of the dielectric layer. Its horizontal force component is independent of the contact angle and acts as a point force on the three-phase contact line. The electrostatic force reduces the contact angle when the electrical potential is applied. The EWOL involves more complex situations: The dielectric film (lotus leaf) is not an equipotential plate. There is a gradient of electrical potential between the two sides of the droplet which results in the asymmetric deformation of droplets to realize the actuation and control of droplets.

The situations of both sides of the lotus leaf will be introduced, respectively. Figure 6 shows the droplet motion of the upside of the lotus leaf and we separate the whole process into two steps:

- **Step 1:** The voltage of the dc electrical source was increased to 150 V.
- **Step 2:** The electrode leaf distance was reduced so the conductive droplet would make contact with the wire electrode. There will be electrical current from the Pt to the counter-electrode through the lotus leaf which generates a gradient of electrical potential in the lotus leaf. The advancing contact angle of the droplet jumps from 154° to 114° due to the application of the electrical potential. This is an unstable process and its characteristic time is of

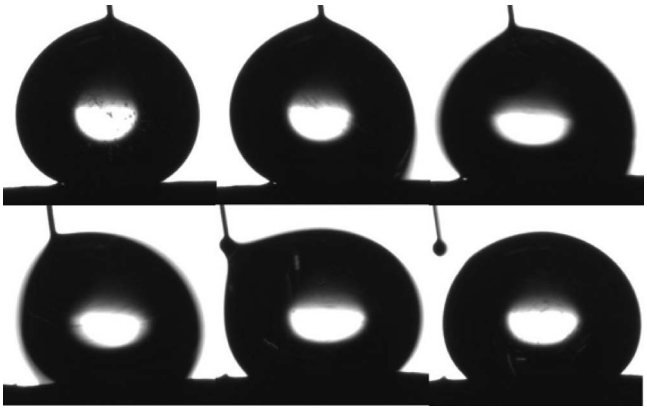

FIG. 6. Voltage-induced droplet motion on the lotus leaf. The interval of each picture is 5 ms.

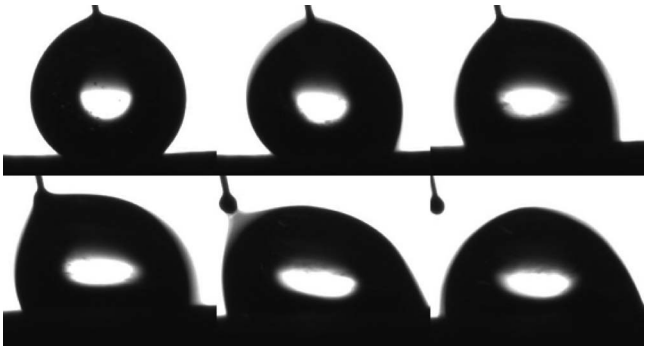

FIG. 7. Voltage-induced droplet motion on the back side of the lotus leaf. The interval of each picture is 5 ms.

the order of 10 ms. A video sequence of this process is shown in Fig. 6, and the interval of each picture is 10 ms. When the droplet settles down totally, the advancing angle recovers from 114° to 124° because the residual charges in the droplet move to the leaf gradually.

Figure 7 shows the situation of the droplet motion induced by applied voltage in the back side of the lotus leaf and we separate the whole process into two steps:

- **Step 1:** The voltage of dc electrical source was increased to 150 V.
- **Step 2:** The electrode leaf distance was reduced so the conductive droplet would make contact with the wire electrode. The advancing contact angle of the droplet jumps from 141° to 79°. A video sequence of this process is shown in Fig. 7, and the interval of each picture is 10 ms. When the droplet ceases to move, the advancing angle shifts from 79° to 96°.

When the applied voltage is larger than 300 V, the droplet sometimes will move two times. The situation when voltage is 400 V is used as example to show the two motions. For simplicity, the whole process was separated into three steps which are shown in Figs. 7 and 8:

- **Step 1:** The voltage of the dc electrical source was increased to 400 V.
- **Step 2:** The electrode leaf distance was reduced so the conductive droplet would make contact with the wire electrode. The contact angle of the droplet jumped from 155° to 104°. A video sequence of this process is shown in Fig. 8, and the interval of each picture is 10 ms. When the droplet stops moving, the advancing angle increases from 104° to 107°.
- **Step 3:** Lift the moving stage so the droplet makes contact with the wire electrode again. The contact angle of the droplet jumps from 107° to 84°. A video sequence of this process is shown in Fig. 9, and the interval of each picture is 10 ms. When the droplet settles down, the

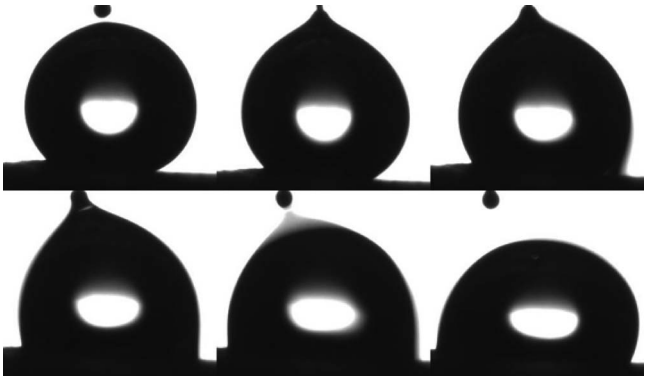

FIG. 8. The first contact of the lotus leaf with the Pt electrode (voltage=400 V). The interval of each picture is 5 ms.

FIG. 9. The second contact of the lotus leaf with the Pt electrode (voltage=400 V). The interval of each picture is 5 ms.

advancing angle changes from 84° to 97° due to the releasing of the residual charge in the droplet.

When the applied voltage increases to 400 V, much heat will be generated. The lotus leaf will be dehydrated by the heat. The appearance of the lotus leaf will change significantly (Fig. 10).

V. ANALYSIS OF RESULTS

The actuating force is the horizontal component of the EW force F_{elec}, and the resistive force includes the viscous resistance F_{viscous}, the contact angle hysteresis F_f, and the drag force applied by the Pt electrode, F_{drag}. The horizontal component of EW force is

$$F_{\text{elec}} \approx 2r\gamma_{lv}(\cos\ \theta_a - \cos\ \theta_r), \tag{2}$$

where r is the radius of the contact area of the droplet and the lotus leaf, the surface tension of droplets is $\gamma_{lv} \approx 72 \times 10^{-3}$ N/m, and θ_a and θ_r are the advancing angle and receding angle with applied voltage, respectively. The advancing angle will decrease with the increase in the applied voltage. In the case of the open EWOD system,[6] the viscous resistance F_{viscous} is described by

$$F_{\text{viscous}} \approx \pi r^2 \tau_w. \tag{3}$$

The shear stress τ_w can be approximately expressed by[6]

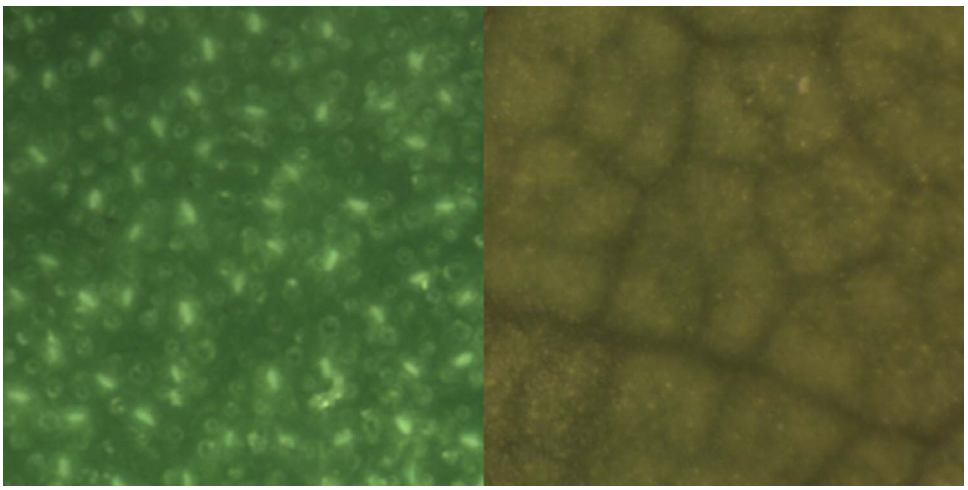

FIG. 10. The lotus leaf before applied 400 V (left); the lotus leaf after applied 400 V (right).

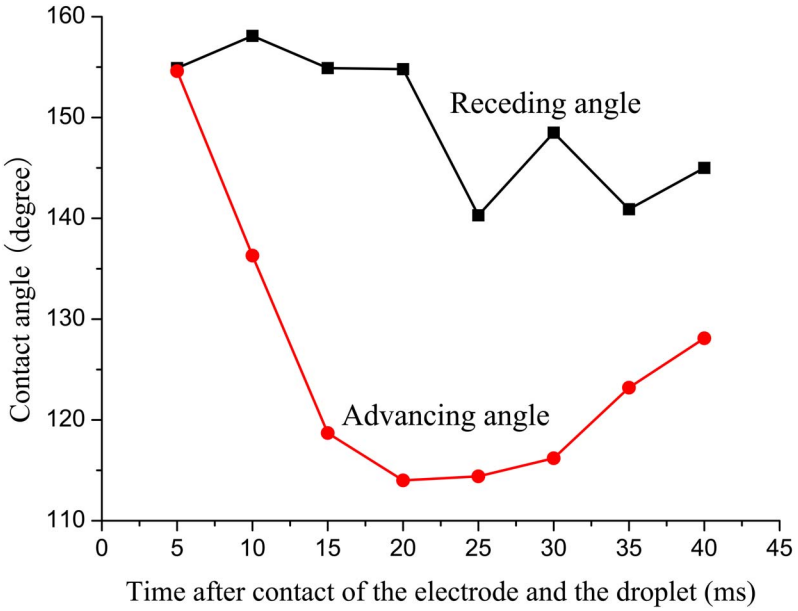

FIG. 11. The relationship between the advancing and receding angles and the time after contact of the droplet and the electrode.

$$\tau_w \approx \frac{5\mu v_{\text{open}}}{2h}, \tag{4}$$

where $h \approx 2$ mm is the height of the droplet and $\mu \approx 0.89 \times 10^{-3}$ Pa s is the viscosity of water at 25 °C. Another resistive force is the force resulting from contact angle hysteresis F_f, which could be estimated by

$$\begin{aligned} F_f &\approx 2r\gamma_{lv}(\cos\,\theta_{r0} - \cos\,\theta_{a0}) \\ &= 4r\gamma_{lv}\,\sin\left(\frac{\theta_{r0}+\theta_{a0}}{2}\right)\sin\left(\frac{\theta_{a0}-\theta_{r0}}{2}\right) \\ &= 4r\gamma_{lv}\,\sin\left(\frac{\theta_{r0}+\theta_{a0}}{2}\right)\sin(1.5^\circ), \end{aligned} \tag{5}$$

where θ_{a0} and θ_{r0} are the advancing and receding angles without applied voltage, respectively. Due to the contact angle hysteresis of the superhydrophobic lotus leaf is only about 3° and $(\theta_{r0}+\theta_{a0})/2$ is about 155°; F_f is much smaller than F_{elec}. The drag force applied by the Pt electrode could be expressed by

$$F_{\text{drag}} \approx \pi D_{\text{Pt}}\gamma_{lv}, \tag{6}$$

where $D_{\text{Pt}} \approx 120$ μm is the diameter of the Pt electrode. The actuation force is $F_a = F_{\text{elec}} - (F_f + F_{\text{viscous}} + F_{\text{drag}}) > 0$, which is enough to fulfill the actuation of the droplet, and the droplet velocity

$$v_{\text{open}} = \int_0^\tau a\,dt \approx \int_0^\tau \frac{F_a(t)}{m}\,dt. \tag{7}$$

Here τ is the actuation time, a is the acceleration generated by the EW force, and m is the mass of the droplet. Figure 11 shows the relationship between the advancing and receding angles and the time after contact of the droplet and the Pt electrode when the applied voltage is 150 V for the

upside of the lotus leaf. So we could get the $F_a(t)$ approximately from Fig. 11. The theoretical result of v_{open} is about 55 mm/s while the experimental result of the speed is about 30 mm/s. The theoretical result could explain the experimental result. It can be seen from Fig. 11 that the advancing angle increases at the end of the motion while the receding contact angle is approximately constant. This is because the droplet separated from the Pt electrode in the end of the motion which opens the electrical circuit as shown in Fig. 7. The electrical current of the open circuit is zero and with the releasing of the residual charges in the droplet the advancing angle increases.

A variety of voltages, including 50, 80, 100, 150, and 400 V, have been tested. It is found that it could fulfill the actuation when the applied voltage is greater than 100 V. When the applied voltage is 50 or 80 V, there will be many bubbles in the droplets without capillary motion. The capacitance of the lotus leaf can be estimated from the actuation criterion,[34]

$$\frac{C}{2\gamma_{lv}}V_{\text{min}}^2 = \frac{\alpha}{1-\alpha}[\sin\ \theta(V_{\text{min}}) + \sin\ \theta_0], \tag{8}$$

where C is the capacitance of the lotus leaf, V_{min} is the minimum electric potential of actuation, and θ_0 is the contact angle of the lotus leaf without applied voltage. In the case where $\theta(V_{\text{min}}) \approx \theta_0$ and α is sufficiently small, Eq. (8) can be simplified as

$$C \approx \frac{4\gamma_{lv}\alpha \sin\ \theta_0}{V_{\text{min}}^2}. \tag{9}$$

From Eq. (9), the capacitance of the lotus leaf, C, is about 0.63 $\mu\text{F/m}^2$.

VI. CONCLUSIONS

The EW experiment on a lotus leaf was carried out for the first time. The capillary motion of the droplet was recorded by a high-speed camera. There is a gradient of electrical potential between the two sides of the droplet which results in the asymmetric deformation of droplets to realize the actuation and control of droplets. The droplets can be actuated in time of the order of 10 ms. This method provides a novel mode to manipulate the droplet. This process is always accompanied by the generation of bubbles, which were brought on by electrolysis and boiling.

ACKNOWLEDGMENTS

This work was jointly supported by the National Basic Research Program of China (973 Program, Grant No. 2007CB310500), National High-tech R&D Program of China (863 Program, Grant Nos. 2007AA04Z348 and 2007AA021803), and National Natural Science Foundation of China (NSFC) (Grant Nos. 10772180 and 10721202). The authors are grateful to Dr. Dong Han of National Center for Nanoscience and Technology of China for the invaluable support on equipments.

[1] O. Sandre, L. Gorre-Talini, A. Ajdari, J. Prost, and P. Silberzan, Phys. Rev. E **60**, 2964 (1999).
[2] M. A. Burns, C. H. Mastrangelo, T. S. Sammarco, F. P. Man, J. R. Webster, B. N. Johnson, B. Foerster, D. Jones, Y. Fields, A. R. Kaiser, and D. T. Burke, Proc. Natl. Acad. Sci. U.S.A. **93**, 5556 (1996).
[3] T. S. Sammarco and M. A. Burns, AIChE J. **45**, 350 (1999).
[4] B. S. Gallardo, V. K. Gupta, F. D. Eagerton, L. I. Jong, V. S. Craig, R. R. Shah, and N. L. Abbott, Science **283**, 57 (1999).
[5] M. Washizu, IEEE Trans. Ind. Appl. **34**, 732 (1998).
[6] J. Berthier, *Microdrops and Digital Microfluidics* (William Andrew, Norwich, NY, 2008).
[7] G. Beni and S. Hackwood, Appl. Phys. Lett. **38**, 207 (1981).
[8] G. Beni and M. A. Tenan, J. Appl. Phys. **52**, 6011 (1981).
[9] M. Vallet, B. Berge, and L. Vovelle, Polymer **37**, 2465 (1996).
[10] W. J. J. Welters and L. G. J. Fokkink, Langmuir **14**, 1535 (1998).
[11] E. Colgate and H. Matsumoto, J. Vac. Sci. Technol. A **8**, 3625 (1990).
[12] W. Dai and Y. P. Zhao, Int. J. Nonlinear Sci. Numer. Simul. **8**, 519 (2007).
[13] J. T. Feng and Y. P. Zhao, J. Phys. D **41**, 052004 (2008).
[14] H. J. J. Verheijen and M. W. J. Prins, Langmuir **15**, 6616 (1999).

[15] H. Moon, S. K. Cho, R. L. Garrell, and C. J. Kim, J. Appl. Phys. **92**, 4080 (2002).
[16] K. T. Kotz, Y. Gu, and G. W. Faris, J. Am. Chem. Soc. **127**, 5736 (2005).
[17] R. D. Sun, A. Nakajima, A. Fujishima, T. Watanabe, and K. Hashimoto, J. Phys. Chem. B **105**, 1984 (2001).
[18] D. Beyssen, L. L. Brizouala, O. Elmazriaa, and P. Alnot, Sens. Actuators B **118**, 380 (2006).
[19] K. L. Wang, T. B. Jones, and A. Raisanen, J. Micromech. Microeng. **17**, 76 (2007).
[20] H. Moona, S. K. Cho, R. L. Garrell, and C. J. Kim, J. Appl. Phys. **92**, 4080 (2002).
[21] M. Abdelgawad, S. L. S. Freire, H. Yang, and A. R. Wheeler, Lab Chip **8**, 672 (2008).
[22] H. S. Chuang, A. Kumar, and S. T. Wereley, Appl. Phys. Lett. **93**, 064104 (2008).
[23] J. Lee, H. Moon, J. Fowler, T. Schoellhammer, and C.-J. Kim, Sens. Actuators, A **95**, 259 (2002).
[24] F. Mugele and J. C. Baret, J. Phys.: Condens. Matter **17**, R705 (2005).
[25] F. Mugele and J. Buehrle, J. Phys.: Condens. Matter **19**, 375112 (2007).
[26] N. Verplanck, Y. Coffinier, V. Thomy, and R. Boukherroub, Nanoscale Res. Lett. **2**, 577 (2007).
[27] N. Verplanck, E. Galopin, J. C. Camart, and V. Thomy, Nano Lett. **7**, 813 (2007).
[28] K. H. Kang, Langmuir **18**, 10318 (2002).
[29] S. L. Ren, S. R. Yang, Y. P. Zhao, T. X. Yu, and X. D. Xiao, Surf. Sci. **546**, 64 (2003).
[30] S. L. Ren, S. R. Yang, and Y. P. Zhao, Acta Mech. Sin. **20**, 159 (2004).
[31] L. Y. Yeo and H. C. Chang, Mod. Phys. Lett. B **19**, 549 (2005).
[32] L. Y. Yeo, R. V. Craster, and O. K. Matar, J. Colloid Interface Sci. **306**, 368 (2007).
[33] L. Y. Yeo and H. C. Chang, Phys. Rev. E **73**, 011605 (2006).
[34] J. Berthier, P. Dubois, P. Clementz, P. Claustre, C. Peponnet, and Y. Fouillet, Sens. Actuators, A **134**, 471 (2007).